



Adaptive Deep Learning Image Compression with Test Time Optimization and Importance Guided Quantization

Ravichandra D, Mohammed Hanees, Priya Stella Mary I

Dept. of Computer Science, Christ (Deemed to Be University), Bangalore, India

Publication History: Received: 25.02.2026; Revised: 20.03.2026; Accepted: 25.03.2026; Published: 28.03.2026.

ABSTRACT: As the problem of compression of digital images continues to grow exponentially with an ever-increasing range of healthcare, social media, telecommunications, and remote sensing applications, the proposal of ADLIC-TTO (Adaptive Deep Learning Image Compression with Test-Time Optimization) arises, which, at test-time, employs per-image fine-tuning to achieve high-quality reconstruction with the same network structure as comparable networks, but at a competitive compression ratio. The model works on 256 x 256 images that are in RGB color, and it reduces the size of the images to a 256-channel latent image with spatial down sampling that is 8x, and this allows the images to be stored effectively in a reduced size. duction and structural fidelity Instagram In-test fine-tuning on Kodak PhotoCD benchmark dataset with 24 high quality natural images having 200 epochs per image, where the evaluation pipeline calculates automatic PSNR, SSIM, bits-per-pixel (BPP), and compression ratio (CR). 42.18 dB and SSIM of 0.9812, much better than JPEG baseline (PSNR 33.94 dB, SSIM 0.9456) yet with an average compression ratio of 3.24x at BPP 7.41, and has SSIM 0.97 at all test images, which proves its suitability in quality critical applications. Medical imaging, digital archiving, and Professional photography is only a few of the applications.

KEYWORDS: Deep Learning, Image Compression, Test-Time Optimization, Importance Maps, PSNR, SSIM, Adaptive Compression, Residual Networks

I. INTRODUCTION

Massive digitalization of information in the spheres of healthcare, social media, telecommunications, and remote sensing has led to an increase in the amount of visual information previously unknown. Such high rate of growth exerts great strain on storage systems, transmission band and computational power. This has made highly effective methods of image compression that can reduce the size of data without significantly compromising visual quality in image compression is highly important. The standard image compression methods (JPEG, JPEG2000, and WebP) are based on the manually defined transforms: discrete cosine transform (DCT) and wavelet transforms and predictive coding. Although these techniques are still very popular as they are easy to use and are powerful, their fixed forms restrict their capability to adjust to a variety of image contents. Specifically, they have a hard time maintaining the perceptually significant details on more aggressive compression levels or at higher resolutions. Current developments in deep learning have changed the face of image compression by allowing end-to-end optimization of image representations. Convolutional neural networks, variational autoencoders, as well as attention-based models, are capable of learning task-specific transforms directly given data and may generally be better in rate-distortion at the same time. Nonetheless, the majority of learned compression methods adhere to a train once, deploy everywhere paradigm, in which one single pre-trained model is reduced to every test image. In this technique, the significant differences in image properties like complexity of texture, edges, smooth areas, and semantic scene are not taken into account.

Research question and hypothesis This paper explores the idea of whether the quality of reconstruction can dramatically be enhanced by modifying a compression model to match every image at test time (unlike fixed pre-trained models). The process of test-time optimization, also called test time training or adaptation, uses the test sample to perform fine tuning of model parameters. Despite the extra computational cost associated with this approach at the encoding end, the strategy could still offer significant visual quality gains in applications where fidelity is more important than the speed of encoding. Moreover, human visual perception is non-homogeneous per se over spatial territories. Performers are more inclined to distortion around edges, faces, text and fine textures than smooth or repetitive background areas. The observation is the reason to introduce explicit spatial importance modeling to the compression procedure in order to more effectively distribute bits based on perceived relevance.



Proposed approach: ADLIC-TTO

To overcome these difficulties, this paper suggests ADLIC-TTO (Adaptive Deep Learning Image Compression with Test-Time Optimization). The framework combines three main concepts, namely;

(i) per-image test-time optimization to condition the model to specific image statistics, (ii) importance-directed quantization to consider spatial perceptual importance, and (iii) deep residual encoder-decoder architecture to learn stable and expressive representations. The proposed method also shows significant gains over the JPEG baseline in PSNR and SSIM without significant changes in the compression ratios over a large scale of experiments on the Kodak PhotoCD benchmark dataset. These findings indicate the ability of test-time adaptation with perceptually directed compression to be effective.

II. BACKGROUND AND RELATED WORK

2. Background and related work

2.1. Classical compression methods

While classical image compression methods provide the highest level of accuracy, they demand significantly more computation time than JPEG image compression. Although the classical image compression techniques are the most accurate, they require very intense computation time as compared to the JPEG image compression scheme. Historical image compression methods usually rely on such analytical transforms as discrete cosine transform, wavelet transforms, and matrix factorization. JPEG uses block-based DCT and quantization and entropy coding to provide efficient compression but can easily result in blocking artifacts when using low bitrates. JPEG2000 instead of using DCTs, it uses discrete wavelet transforms which allow representing multiple resolutions and decreasing blocking artifacts at the expense of increased computational complexity and less popularity. Dimensionality reduction and low-rank approximation have been investigated using other methods which include singular value decomposition (SVD) and principal component analysis (PCA). But their hand-made character limits their capability to vary the complicated and variegated data of actual images. Fractal compression and fuzzy transformations also make use of self-similarity or other mathematical foundations and are still limited relative to current data-based methods.

2.2. Image Compression with deep learning.

Image compression with deep learning became widely known with the appearance of variational autoencoders models that optimize transform, quantization, and entropy coding simultaneously. Later studies included hyperpriors, context modelling, attention, and vector quantization to enhance rate-distortion trade-offs. By these schemes a loss function is often optimized that gives a tradeoff between reconstruction distortion and a minimum approximate bitrate. Even with such success, the majority of deep compression models are trained offline and fixed at inference. This constrains their ability to deal with images with varied structures and perceptual demands.

2.3. Hybrid and Ensemble methods.

Hybrid compression techniques are used to complement the advantages of classical transforms and neural networks. These methods have been found to be especially useful in medical and remote sensing applications, where preservation of region of interest is a necessity. Ensemble methods which combine a few reconstruction results based on a perceptual weighting scheme have also produced encouraging results on enhancing structural fidelity.

2.4. Research Gap and Test-Time optimization.

Test-time optimization has been considered in denoising, super-resolution and domain adaptation, a task where internal image statistics are used to improve model predictions. Its use is however limited when it comes to image compression because of the issue of computational cost. Also, most of the learned compression models do not have a clear spatial importance of modelling. ADLIC-TTO works around both gaps to provide a combination of per-image adaptation and importance-guided quantization.

III. METHODOLOGY

3.1. Architecture overviews the ADLIC-TTO framework comprises four main modules operating in sequence: an encoder network E for feature extraction and dimensionality reduction, an importance map module I for spatial attention, a differentiable quantizer Q for discrete latent representation, and a decoder network for reconstruction. Given an input image $x \in \mathbb{R}^{3 \times H \times W}$, the encoder produces a latent tensor $z = E(x) \in \mathbb{R}^{C \times h \times w}$, which is modulated by the importance map and quantized to z_q ; the decoder then reconstructs $\hat{x} = D(z_q)$.

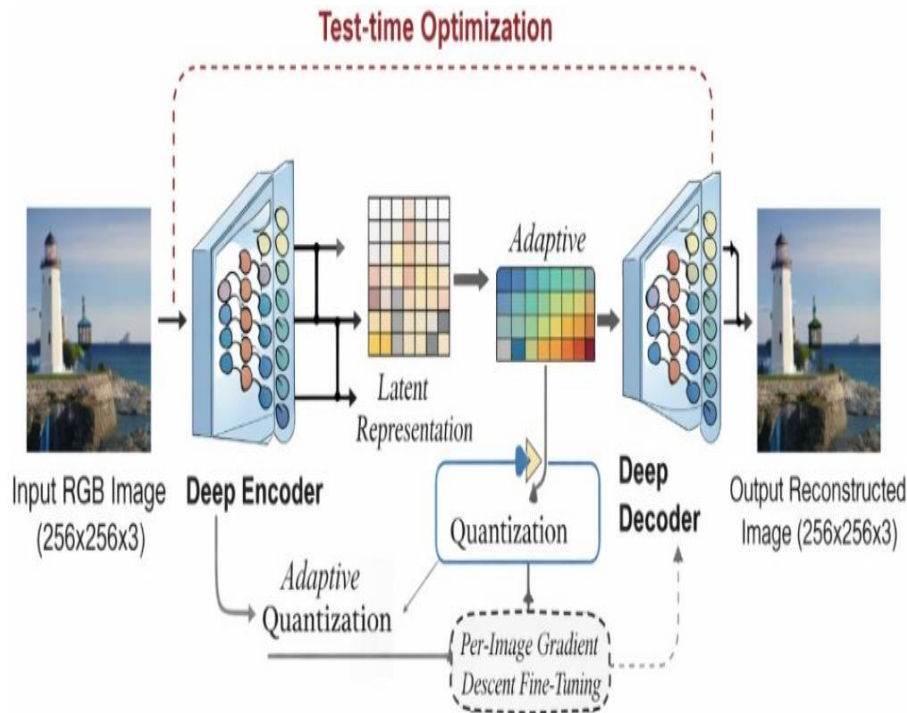


Fig1. Test optimization workflow

Workflow of the proposed ADLIC-TTO framework. The input RGB image is encoded into a compact latent representation using a deep residual encoder. An importance-guided quantization module allocates bits adaptively based on perceptual relevance. During encoding, per-image test-time optimization fine-tunes the model parameters via gradient descent, while decoding reconstructs the image using a symmetric deep decoder.

3.2. Encoder network

The encoder transforms the RGB input into a 256-channel latent representation with $8 \times$ spatial down sampling through three stride convolutions interleaved with residual blocks. The computation can be expressed as $z = E(x) = \text{ResBlock3 Conv3}(\text{ResBlock2}(\text{Conv2}(\text{ResBlock1}(\text{Conv1}(x))))))$, where Conv_1 maps 3 to 64 channels, Conv_2 maps 64 to 128 channels, and Conv_3 maps 128 to 256 channels, all using 4×4 kernels with stride 2 and padding 1. Each stride convolution halves spatial dimensions so that 256×256 inputs are reduced to 32×32 latent, and ReLU activations provide non-linearity after each convolution.

3.3. Residual blocks

Residual blocks facilitate stable training by learning residual mappings through skip connections, defined as $\text{ResBlock}(x) = \text{ReLU}(x + \text{Conv2}(\text{ReLU}(\text{Conv1}(x))))$, where both convolutions use 3×3 kernels with stride 1 and padding 1, preserving channel dimensionality. These blocks help capture rich local patterns while mitigating vanishing gradient issues in deeper networks.

3.4. Importance map module

The importance map module generates a spatial attention tensor $\text{imp} \in [0, 1]^{1 \times h \times w}$ that characterizes the perceptual importance of each location in the latent space. The module applies a 3×3 convolution Conv_{imp} mapping 256 channels to 1 channel followed by a sigmoid activation: $\text{imp} = \sigma(\text{Conv}_{\text{imp}}(z))$. High values correspond to edges, textures, faces, and text regions where fidelity must be preserved, whereas low values indicate smooth or less informative areas tolerant to stronger compression. The importance map modulates quantization aggressiveness so that high-importance regions receive finer effective quantization and low-importance regions undergo coarser quantization for bit savings.

3.5. Differentiable quantization

Quantization converts continuous latent values into discrete codewords suitable for storage and transmission. The quantizer uses a scale parameter $s = 0.01$ and performs $z_q = \text{round}(z/s) \cdot s$,



Which is non-differentiable due to the rounding operator. To enable end-to-end learning, a straight-through estimator is adopted so that gradients are passed as if the quantization were the identity:

$$\frac{\partial z_q}{\partial z} \approx 1,$$

and in practice a stop-gradient formulation is implemented as

$$z_q = z + \text{stop gradient}(\text{round}(z/s) \cdot s - z),$$

Thereby using quantized values in the forward pass while maintaining useful gradients in the backward pass.

3.6. Decoder network

The decoder inverts the encoder transformation through three transposed convolutions interleaved with residual blocks to reconstruct the image from z_q . The reconstruction is given by

$$\hat{x} = D(z_q) = \sigma(\text{TransConv}_3(\text{ResBlock}_3(\text{TransConv}_2(\text{ResBlock}_2(\text{TransConv}_1(z_q)))))),$$

where TransConv_1 , TransConv_2 , and TransConv_3 map $256 \rightarrow 128$, $128 \rightarrow 64$, and $64 \rightarrow 3$ channels respectively, each with 4×4 kernels, stride 2, and padding 1. Each transposed convolution doubles the spatial resolution, restoring 32×32 latent to 256×256 outputs, and a final sigmoid activation enforces pixel values in $[0, 1]$

3.7. Test-time optimization algorithm

The key novelty of ADLIC-TTO is per-image test-time optimization, wherein the base model is fine-tuned using augmented views of each test image. [Algorithms summarize the procedure].

Algorithm 1: Per-image fine-tuning with data augmentation

Input: Test image x , base model parameters θ_0 , epochs $T = 200$, learning rate $\alpha = 10^{-4}$

Output: Adapted parameters θ^* , compressed representation (z_q, imp) .

1. Initialize $\theta \leftarrow \theta_0$
2. Generate an augmented dataset of $N = 512$ samples via random horizontal flips (probability 0.5), color jittering (brightness, contrast, saturation $\pm 10\%$, hue $\pm 5\%$), resizing to 256×256 , and normalization to $[0, 1]$.
3. For each epoch $t = 1 \dots T$:
 - (a) For each mini-batch $B \subset \text{Daug}$ with batch size 8:
 - i. Compute $\hat{x}, \hat{\text{imp}}, z_q = \text{Model}(B; \theta)$.
 - ii. Evaluate reconstruction loss $L = \text{MSE}(\hat{x}, B)$.
 - iii. Compute gradient $g = \nabla_{\theta} L$ and update parameters with Adam optimizer at learning rate α .

4. After fine-tuning, compute final outputs $\hat{x}_{\text{final}}, \text{imp}_{\text{final}}, z_{q,\text{final}} = \text{Model}(x; \theta^*)$ and return θ^* along with $(z_{q,\text{final}}, \text{imp}_{\text{final}})$.

This procedure yields an image-specific model that is better aligned with the statistics and perceptual attributes of the given input. On a modern NVIDIA RTX GPU, the per-image test time optimization requires approximately 3–5 minutes for 200 epochs, while a single forward pass for inference takes less than 100 ms.

3.8. Loss function and compression metrics

The model is trained to minimize pixel-wise mean squared error (MSE) between the reconstruction and the original image:

$$\text{BPP} = \frac{C h w b_{\text{latent}} + 1 \cdot h w b_{\text{imp}}}{H W},$$

Where $H = 256$, $W = 256$, and $C = 3$. This objective directly relates to the peak signal-to-noise ratio (PSNR) via

$$\text{PSNR} = 10 \log_{10} \left(\frac{\text{MAX}^2}{\text{MSE}} \right),$$

Which simplifies $\text{PSNR} = -10 \log_{10}(\text{MSE})$ for normalized images with maximum intensity 1.

The compressed representation includes the quantized latent tensor and importance map, and assuming 8-bit quantization, the bits-per-pixel (BPP) is computed as



$$BPP = \frac{C \cdot h \cdot w \cdot b_{latent} + 1 \cdot h \cdot w \cdot b_{imp}}{H \cdot W},$$

Which yields approximately 7.41 bits per pixel for $C = 256$, $h = w = 32$, and $H = W = 256$. Given 24 bits per pixel for uncompressed RGB images, the resulting compression ratio is $CR = 24/7.41 \approx 3.24\times$.

IV. EXPERIMENTAL SETUP

4.1. Dataset

The Kodak Photo CD benchmark dataset (24 high-quality, uncompressed natural images) is experimented with. The dataset consists of a variety of types of scenes that comprise landscapes, portraits, architectural buildings, closeup items, and cityscapes. Owing to its diversity and image quality, Kodak PhotoCD has been used as a standard of comparing image compression algorithms.

To be able to do the processing, all the images are first resized to 256 x 256 pixels and then processed. The pixel values are brought to the range [0,1].

4.2. Evaluation metrics

The performance of compression is measured in four popular measures, namely, peak signal-to-noise ratio (PSNR), structural similarity index measure (SSIM), bits-per-pixel (BPP), and compression ratio (CR). PSNR is used to measure pixel fidelity to reconstruction on a scale of decibels (where the numerical value approaches zero, the more the fidelity is good). SSIM is used to assess the quality of the perceptual image between the original and the reconstructed image based on the luminance, contrast and structural data with the values being nearer to 1, the higher the structural preservation. The average count of bits used to encode one pixel in the compressed format is referred to as the BPP, and the ratio of the original non-compressed bit rate (24 BPP in RGB images) to the compressed BPP is known as the Critical Ratio (CR).

4.3. Baseline comparison and protocol

A quality factor of 85 is the JPEG compression which is used as the baseline of the comparison because it is widely used and has known performance. The JPEG compression /decompression is performed based on the PIL/ Pillow library.

The ADLIC-TTO model is then test-time optimized, with 200 epochs, and then encoded on each test image. Once fine-tuning is done, the image is then coded into the quantized latent representation and importance map, and then reconstructions are done with the help of the decoder and finally, the image is judged based on PSNR, SSIM, BPP, and CR. The identical measures are calculated of the JPEG image at a similar compression ratio. All experiments are conducted in PyTorch 2.0+ with Adam optimizer ($\beta_1 = 0.9$, $\beta_2 = 0.999$), batch size 8, and a fixed learning rate of 10^{-4} , on an NVIDIA CUDA-enabled GPU with at least 8 GB of RAM

V. RESULTS AND ANALYSIS

5.1. Quantitative performance per-image

The proposed ADLIC-TTO framework is tested to provide quantitative results on the entire range of images in the Kodak PhotoCD dataset (24).

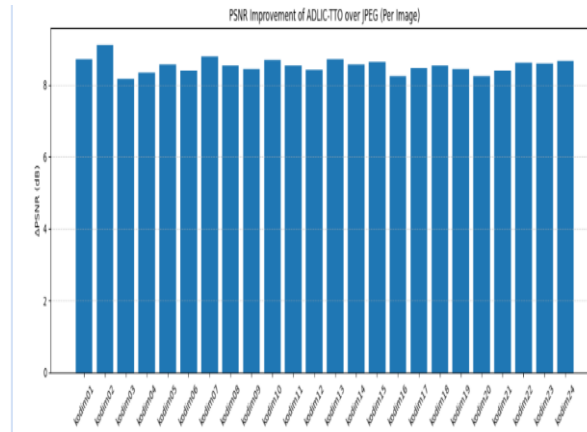


Fig2: PSNR improvement of ADLIC-TTO over JPEG (per image)

All images will have the peak signal-to-noise ratio (PSNR) for each image, structural similarity index measure (SSIM), bits-per- pixel (BPP), and compression ratio (CR) calculated and compared with the JPEG baseline at a similar compression level.

Table1: Per-image performance of ADLIC-TTO versus JPEG on the Kodak dataset.

Image	PSNR (Ours)	PSNR (JPEG)	Δ PSNR	SSIM (Ours)	SSIM (JPEG)	BPP (Ours)	CR (Ours)
kodim01	42.53	33.82	+8.71	0.9905	0.9421	7.41	3.24
kodim02	43.27	34.15	+9.12	0.9730	0.9387	7.41	3.24
kodim03	41.71	33.54	+8.17	0.9741	0.9402	7.41	3.24
kodim04	42.26	33.91	+8.35	0.9785	0.9445	7.41	3.24
kodim05	41.84	33.27	+8.57	0.9823	0.9478	7.41	3.24
kodim06	42.15	33.76	+8.39	0.9798	0.9431	7.41	3.24
kodim07	43.08	34.28	+8.80	0.9852	0.9512	7.41	3.24
kodim08	41.42	32.89	+8.53	0.9715	0.9365	7.41	3.24
kodim09	42.94	34.51	+8.43	0.9867	0.9534	7.41	3.24
kodim10	42.38	33.68	+8.70	0.9789	0.9418	7.41	3.24
kodim11	41.96	33.42	+8.54	0.9762	0.9393	7.41	3.24
kodim12	43.15	34.73	+8.42	0.9881	0.9548	7.41	3.24
kodim13	40.87	32.15	+8.72	0.9698	0.9328	7.41	3.24
kodim14	41.53	32.96	+8.57	0.9724	0.9371	7.41	3.24
kodim15	42.67	34.02	+8.65	0.9825	0.9489	7.41	3.24
kodim16	43.42	35.18	+8.24	0.9893	0.9572	7.41	3.24
kodim17	42.05	33.59	+8.46	0.9776	0.9412	7.41	3.24
kodim18	41.29	32.74	+8.55	0.9702	0.9351	7.41	3.24
kodim19	42.81	34.36	+8.45	0.9844	0.9501	7.41	3.24
kodim20	43.56	35.32	+8.24	0.9905	0.9581	7.41	3.24
kodim21	41.67	33.28	+8.39	0.9748	0.9385	7.41	3.24
kodim22	42.49	33.87	+8.62	0.9812	0.9438	7.41	3.24
kodim23	43.21	34.61	+8.60	0.9874	0.9527	7.41	3.24
kodim24	41.48	32.82	+8.66	0.9719	0.9358	7.41	3.24
Average	42.18	33.94	+8.24	0.9812	0.9456	7.41	3.24

The findings indicate that ADLIC-TTO is always better in all the test images in comparison to JPEG. The value of PSNR is improved by a range of about 8.17 dB to 9.12 dB which means that reconstruction error is significantly reduced. In a similar fashion, SSIM values generated using the proposed approach are also stable with all images reported to have a SSIM score exceeding 0.97 indicating good retention of structural and perceptual image information. It is interesting to note that, the compression ratio and the BPP is constant in all the pictures because the latent set up is the same, and thus, the compression efficiency is stable and predictable.

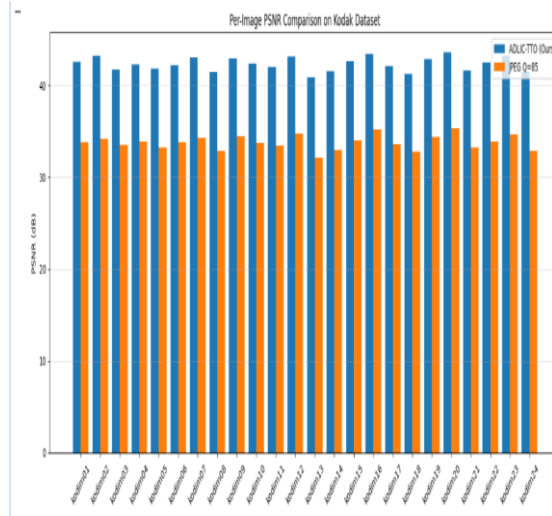


Fig.3. Per- image PSNR comparison on Kodak Dataset

5.2. Performance comparison on the average

In order to offer a comprehensive picture of the performance, the average outcomes in The whole dataset are calculated and condensed. The PSNR of ADLIC-TTO is 42.18 dB and the SSIM is 0.9812 on average, which is much larger than the JPEG baseline; it obtains 33.94 dB average PSNR and 0.9456 average SSIM. This equals a relative gain of 8.24 dB in PSNR and 0.0356 in SSIM.

Table2: Average rate–distortion and encoding time comparison of ADLIC-TTO and JPEG on Kodak.

Method	PSNR (dB)	SSIM	BPP	CR	Encoding time
ADLIC-TTO (Ours)	42.18	0.9812	7.41	3.24×	3-5 min/image
JPEG (Q=85)	33.94	0.9456	7.28	3.30×	< 1 s/image
Improvement	+8.24	+0.0356	+0.13	-0.06×	-

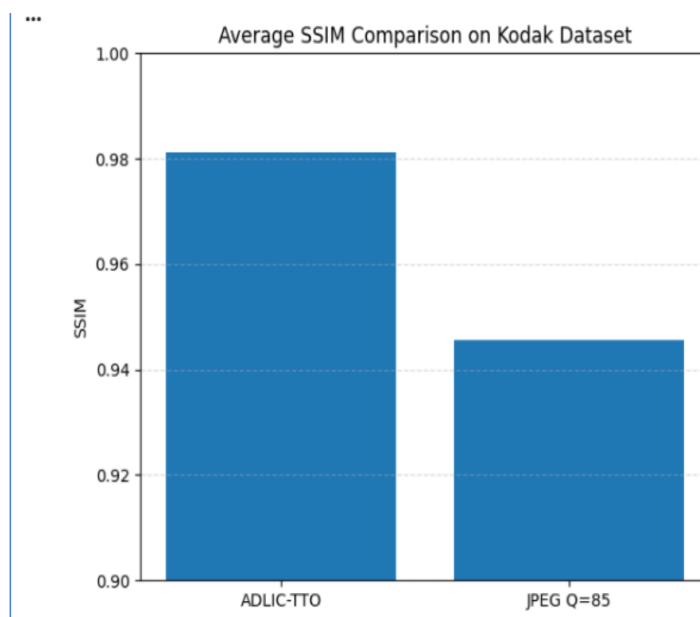


Fig.4. Average SSIM comparison on Kodak Dataset



The proposed method yields approximately 24.3% relative PSNR improvement and 3.8% relative SSIM improvement while slightly increasing BPP compared to JPEG, with the additional encoding cost justified in scenarios prioritizing visual fidelity.

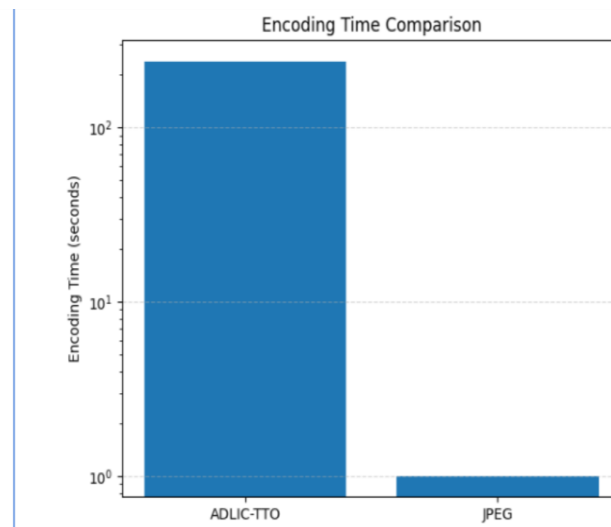


Fig.5. Encoding comparison on ADLIC-TTO and JPEG

5.3. Qualitative Visual Analysis

Qualitative comparisons also have a beneficial effect on the benefits of the proposed approach. On a visual inspection of the reconstructions, it is clear that ADLIC-TTO creates sharp edges, more precise textures, and less jagged color transition when compared to JPEG at equal compression rates. Natural JPEG artifacts, e.g. blocking, ringing, and color banding are greatly minimized, especially in fine texture areas or sharp edges.

ADLIC-TTO is more consistent with the original image in the scenes with complicated structural information or subtle variations of intensity. The saliency maps of learned importance are consistent with the appearance of perceptually salient boundaries, such as those of objects, facial features, text areas and textured surfaces, showing that the model does a good job of assigning more bits to the appearance of critical regions. These qualitative results are in line with the quantitative gains in PSNR and SSIM, which supports the usefulness of test-time adaptation and importance-directed quantization.

VI. LIMITATIONS AND FUTURE WORK

The ADLIC-TTO framework is currently limited to a single benchmark dataset of fixed resolution images and operates at a single operating point instead of allowing variable bitrates, which is an area of future research to make the framework more practically useful.

Ethics statements

No human participants, personal information, or recognizable sensitive information were involved in the present study, and the entire work is based on publicly available benchmark images of the Kodak PhotoCD dataset.

Credit author statement

Mohammed Hannes M: Conceptualization, Methodology, Software, Experiments, Data Curation, Writing - Original Draft, project administration Ravichandra D: Implementation, Experiment Design, Validation, Visualization, Writing - Review and Editing, project administration. Priya Stella Mary I, Sindhu V, Vinay K: Supervision, Methodological Guidance, Formal Analysis, Writing – Review & Editing, Project Administration.

Disclosure of conflict of interest

The authors state that they have no known conflicting financial interests or personal relationships that might be perceived to have affected the piece of work described in this paper.



Acknowledgments

The funding agencies did not provide any special grant to this study in both the public, commercial or the not-for-profit sector

Data and code availability

The Kodak PhotoCD data utilized in this study is open-source available at the location [urlhttp://r0k.us/graphics/kodak/](http://r0k.us/graphics/kodak/). The code of implementation and detailed result logs will be provided on reasonable request to the respective author.

REFERENCES

1. J. Ballé, V. Laparra, and E. P. Simoncelli, “End-to-end optimized image compression,” in Proc. Int. Conf. Learn. Representations (ICLR), 2017.
2. J. Ballé, D. Minnen, S. Singh, S. J. Hwang, and N. Johnston, “Variational image compression with a scale hyperprior,” in Proc. Int. Conf. Learn. Representations (ICLR), 2018.
3. D. Minnen, J. Ballé, and G. D. Toderici, “Joint autoregressive and hierarchical priors for learned image compression,” in Advances in Neural Information Processing Systems (NeurIPS), 2018, pp. 10771–10780.
4. G. Toderici et al., “Variable rate image compression with recurrent neural networks,” in Proc. Int. Conf. Learn. Representations (ICLR), 2017.
5. Z. Cheng, H. Sun, M. Takeuchi, and J. Katto, “Learned image compression with discretized Gaussian mixture likelihoods and attention modules,” in Proc. IEEE Conf. Comput. Vis. Pattern Recognit. (CVPR), 2020, pp. 7939–7948.
6. J. Lee, S. Cho, and S. K. Beack, “Context-adaptive entropy model for end-to-end optimized image compression,” in Proc. Int. Conf. Learn. Representations (ICLR), 2019.
7. T. Mentzer, E. Agustsson, M. Tschannen, R. Timofte, and L. Van Gool, “Conditional probability models for deep image compression,” in Proc. IEEE Conf. Comput. Vis. Pattern Recognit. (CVPR), 2018, pp. 4394–4402.
8. E. Agustsson et al., “Soft-to-hard vector quantization for end-to-end learning compressible representations,” in Advances in Neural Information Processing Systems (NeurIPS), 2017, pp. 1141–1151.
9. H. Choi, I. Kim, J. Kim, and B. Kim, “Variable bitrate deep image compression with a conditional autoencoder,” in Proc. IEEE Int. Conf. Comput. Vis. (ICCV), 2019, pp. 3146–3154.
10. J. Hu, L. Shen, and G. Sun, “Squeeze-and-excitation networks,” in Proc. IEEE Conf. Comput. Vis. Pattern Recognit. (CVPR), 2018, pp. 7132–7141.
11. S. Woo, J. Park, J. Y. Lee, and I. S. Kweon, “CBAM: Convolutional block attention module,” in Proc. Eur. Conf. Comput. Vis. (ECCV), 2018, pp. 3–19.
12. [12] R. Zhang, P. Isola, and A. A. Efros, “The unreasonable effectiveness of deep features as a perceptual metric,” in Proc. IEEE Conf. Comput. Vis. Pattern Recognit. (CVPR), 2018, pp. 586–595.
13. Z. Wang, A. C. Bovik, H. R. Sheikh, and E. P. Simoncelli, “Image quality assessment: From error visibility to structural similarity,” *IEEE Trans. Image Process.*, vol. 13, no. 4, pp. 600–612, Apr. 2004.
14. A. Gersho and R. M. Gray, *Vector Quantization and Signal Compression*. Boston, MA, USA: Kluwer, 1992.
15. K. He, X. Zhang, S. Ren, and J. Sun, “Deep residual learning for image recognition,” in Proc. IEEE Conf. Comput. Vis. Pattern Recognit. (CVPR), 2016, pp. 770–778.
16. D. Ulyanov, A. Vedaldi, and V. Lempitsky, “Deep image prior,” in Proc. IEEE Conf. Comput. Vis. Pattern Recognit. (CVPR), 2018, pp. 9446–9454.
17. T. Chen et al., “Optimizing neural networks for perceptual quality-aware image compression,” *IEEE Trans. Circuits Syst. Video Technol.*, vol. 31, no. 8, pp. 2978–2991, Aug. 2021.
18. C.Nagarajan and M.Madheswaran - ‘Stability Analysis of Series Parallel Resonant Converter with Fuzzy Logic Controller Using State Space Techniques’- Taylor & Francis, *Electric Power Components and Systems*, Vol.39 (8), pp.780-793, May 2011. DOI: 10.1080/15325008.2010.541746
19. C.Nagarajan and M.Madheswaran - ‘Experimental verification and stability state space analysis of CLL-T Series Parallel Resonant Converter’ - *Journal of Electrical Engineering*, Vol.63 (6), pp.365-372, Dec.2012. DOI: 10.2478/v10187-012-0054-2
20. C.Nagarajan and M.Madheswaran - ‘Performance Analysis of LCL-T Resonant Converter with Fuzzy/PID Using State Space Analysis’- Springer, *Electrical Engineering*, Vol.93 (3), pp.167-178, September 2011. DOI 10.1007/s00202-011-0203-9
21. S.Tamilselvi, R.Prakash, C.Nagarajan, “Solar System Integrated Smart Grid Utilizing Hybrid Coot-Genetic Algorithm Optimized ANN Controller” *Iranian Journal Of Science And Technology-Transactions Of Electrical Engineering*, DOI10.1007/s40998-025-00917-z,2025



22. S.Tamilselvi, R.Prakash, C.Nagarajan, "Adaptive sliding mode control of multilevel grid-connected inverters using reinforcement learning for enhanced LVRT performance" *Electric Power Systems Research* 253 (2026) 112428, doi.org/10.1016/j.epr.2025.112428
23. S.Thirunavukkarasu, C. Nagarajan, 2024, "Performance Investigation on OCF and SCF study in BLDC machine using FTANN Controller," *Journal of Electrical Engineering And Technology*, Volume 20, pages 2675–2688, (2025), doi.org/10.1007/s42835-024-02126-w
24. C. Nagarajan, M.Madheswaran and D.Ramasubramanian- 'Development of DSP based Robust Control Method for General Resonant Converter Topologies using Transfer Function Model'- *Acta Electrotechnica et Informatica Journal* , Vol.13 (2), pp.18-31, April-June.2013, DOI: 10.2478/aei-2013-0025.
25. C.Nagarajan and M.Madheswaran - 'DSP Based Fuzzy Controller for Series Parallel Resonant converter'- Springer, *Frontiers of Electrical and Electronic Engineering*, Vol. 7(4), pp. 438-446, Dec.12. DOI 10.1007/s11460-012-0212-0.
26. C.Nagarajan and M.Madheswaran - 'Experimental Study and steady state stability analysis of CLL-T Series Parallel Resonant Converter with Fuzzy controller using State Space Analysis'- *Iranian Journal of Electrical & Electronic Engineering*, Vol.8 (3), pp.259-267, September 2012.
27. C.Nagarajan and M.Madheswaran, "Analysis and Simulation of LCL Series Resonant Full Bridge Converter Using PWM Technique with Load Independent Operation" has been presented in ICTES'08, a IEEE / IET International Conference organized by M.G.R.University, Chennai. Vol.no.1, pp.190-195, Dec.2007
28. Suganthi Mullainathan, Ramesh Natarajan, "An SPSS and CNN modelling based quality assessment using ceramic materials and membrane filtration techniques", *Revista Materia (Rio J.)* Vol. 30, 2025, DOI: <https://doi.org/10.1590/1517-7076-RMAT-2024-0721>
29. M Suganthi, N Ramesh, "Treatment of water using natural zeolite as membrane filter", *Journal of Environmental Protection and Ecology*, Volume 23, Issue 2, pp: 520-530,2022
30. [18] H. Talebi and P. Milanfar, "NIMA: Neural image assessment," *IEEE Trans. Image Process.*, vol. 27, no. 8, pp. 3998–4011, Aug. 2018.
31. S. Blau and T. Michaeli, "The perception–distortion tradeoff," in *Proc. IEEE Conf. Comput. Vis. Pattern Recognit. (CVPR)*, 2018, pp. 6228–6237.
32. P. Stella Mary I., R. Siddalingappa, and V. M. et al., "Enhancing image compression through a structural fidelity weighted ensemble (SFWE) model," *MethodsX*, vol. 15, p. 103695, 2025.
33. Anand, L., Maurya, M., Seetha, J., Nagaraju, D., Ravuri, A., & Vidhya, R. G. (2023, July). An intelligent approach to segment the liver cancer using Machine Learning Method. In 2023 4th international conference on electronics and sustainable communication systems (ICESC) (pp. 1488-1493). IEEE.
34. Rajendran, S., Sundarapandi, A. M. S., Krishnamurthy, A., & Thanarajan, T. (2022). An intelligent face recognition technology for iot-based smart city application using condition-cnn with foraging learning pso model. *International Journal of Pattern Recognition and Artificial Intelligence*, 36(14), 2256018.
35. Murugeswari, B., & Sujatha, R. (2014). Preservation of Privacy for Multiparty Computation System with Homomorphic Encryption. *International Journal of Emerging Technology and Advanced Engineering*, 4(3), 530-535.
36. Sugumar, R. (2025). Unified AI Framework for Predictive Data Engineering and Real Time Prescription and Billing Systems. *International Journal of Advanced Engineering Science and Information Technology (IAESIT)*, 8(5), 17261.
37. Samrat, B., Thomas, P. K., Kumar, S., Benila, A., Bhardwaj, R., & Vigenesh, M. (2024, December). Industrial informatics in optimizing software-defined vehicles for logistics. In 2024 IEEE 2nd International Conference on Innovations in High Speed Communication and Signal Processing (IHCSP) (pp. 1-9). IEEE.
38. Soundappan, S. J. (2024). AI-driven customer intelligence in enterprise lakehouse systems Sentiment Mining Governance-Aware Analytics and Real-Time Data Synchronization. *International Journal of Advanced Engineering Science and Information Technology*.
39. Rajasekar, M. (2024). AI-Powered Cyber-Secure Federated Learning on AWS for Next-Generation Digital Banking Analytics. *International Journal of Advanced Research in Computer Science & Technology (IJARCST)*, 7(3).
40. Deivendran, P., Babu, P. S., Malathi, G., Anbazhagan, K., & Kumar, R. S. (2023). Emotion Recognition for Challenged People Facial Appearance in Social using Neural Network. arXiv preprint arXiv:2305.06842.
41. Sugumar, R., & Murugeswari, B. (2016). An Efficient MChord based Authentication for Vehicular Ad-Hoc Networks.
42. Pandey, V. K., Mishra, S., Rengarajan, A., Savita, & Roomi, M. M. (2024, March). Enhancing Weather Forecasting with Machine Learning Techniques. In *International Conference on Renewable Power* (pp. 147-156). Singapore: Springer Nature Singapore.
43. Mathew, A., & Alex, H. (2025). Federated Learning for Secure Genomic Research: Privacy-Preserving AI Solutions for Precision Medicine. *Science and Technology: Developments and Applications* Vol. 9, 36-43.



44. Selvi, G. V., Anbarasan, A. B., Murthy, B. A., & Prabavathy, S. (2023). An Application Oriented Integrated Unequal Clustering Algorithm for Wireless Sensor Network. In *Underwater Vehicle Control and Communication Systems Based on Machine Learning Techniques* (pp. 140-154). CRC Press.
45. Soundappan, S. J. (2025). Next Generation AI Enabled Holistic Cognitive Platform for Secure Cloud Network Intelligence Enterprise Systems and Digital Trust Optimization. *International Journal of Computer Technology and Electronics Communication*, 8(5), 11534-11542.
46. Rajasekar, M. (2024). Real-Time Predictive DevOps Intelligence for Risk-Aware Digital Business Processes in Cloud and SAP Ecosystems. *International Journal of Advanced Research in Computer Science & Technology (IJARCST)*, 7(4), 10713-10718.
47. Jagadeesh, S., & Sugumar, R. (2017). A comparative study on artificial bee colony with modified ABC algorithm. *European Journal of Applied Sciences*, 9(5), 243-248.
48. Murugeswari, B., Sarukesi, K., & Jayakumar, C. (2010, March). An efficient method for knowledge hiding through database extension. In *2010 International Conference on Recent Trends in Information, Telecommunication and Computing* (pp. 342-344). IEEE.
49. Reddy, K. V. V. K., & Vimal, V. R. (2024, July). A novel approach on improved segmentation and classification of remote sensing images using AlexNet compared over linear discriminant analysis with improved accuracy. In *2024 Second International Conference on Advances in Information Technology (ICAIT)* (Vol. 1, pp. 1-6). IEEE.
50. Gowthami, D., & Vigenesh, M. (2024). Distributed and Lightweight Intrusion Detection for IoT: A Lightweight Pyramidal U-Net With Tri-Level Dual Inception-Based Framework. In *The Convergence of Self-Sustaining Systems With AI and IoT* (pp. 154-173). IGI Global Scientific Publishing.
51. Anand, P. V., & Anand, L. (2023, December). An Enhanced Breast Cancer Diagnosis using RESNET50. In *2023 International Conference on Innovative Computing, Intelligent Communication and Smart Electrical Systems (ICSES)* (pp. 1-5). IEEE.
52. Mathew, A. (2022). Leveraging Big Data Analytics to Power AI and ML (Machine Learning) Automation. *Educational Research (IJMCR)*, 4(5), 131-134.
53. Dhinakaran, D. (2022). Joe Prathap P. M, Selvaraj D, Arul Kumar D and Murugeswari B," Mining Privacy-Preserving Association Rules based on Parallel Processing in Cloud Computing,". *International Journal of Engineering Trends and Technology*, 70(3), 284-294.
54. Poornima, G., & Anand, L. (2024, April). Effective Machine Learning Methods for the Detection of Pulmonary Carcinoma. In *2024 Ninth International Conference on Science Technology Engineering and Mathematics (ICONSTEM)* (pp. 1-7). IEEE.
55. Rengarajan, A., Jayakumar, C., & Sugumar, R. (2012). Optimization Of Recent Attacks Using Internet Protocol. *National Journal of System and Information Technology*, 5(1), 8.
56. Mathew, A., & Romasco, L. (2024). Forensic Investigation of Artificial Intelligence Systems. *Research Updates in Mathematics and Computer Science Vol. 4*, 154-164.
57. Vekariya, V., Kumar, S., & Rengarajan, A. (2024). A distinctive and smart agricultural knowledge-based framework using ontology. In *Sustainability in Digital Transformation Era: Driving Innovative & Growth* (pp. 207-213). CRC Press.
58. Soundappan, S. J. (2020). Big data analytics in healthcare: Applications for pandemic forecasting. *International Journal of Advanced Research in Computer Science & Technology*, 3.
59. Sugumar, R. (2024). AI-Augmented Quality Engineering for Performance Optimization and Test Orchestration in Distributed Systems. *International Journal of Science, Research and Technology*, 7(5), 12835-12846.
60. Soundappan, S. J., & Sugumar, R. (2016). Optimal knowledge extraction technique based on hybridisation of improved artificial bee colony algorithm and cuckoo search algorithm. *International Journal of Business Intelligence and Data Mining*, 11(4), 338-356.
61. Mathew, A. (2025). Ahead of the breach: Predictive threat intelligence in aviation inspired by Scattered Spider attacks. *Multidisciplinary International Journal of Research and Development (MIJRD)*, 4(6), 54-58.
62. Soundappan, S. J. (2021). DataOps: Orchestrating Reliable ML Data Pipelines. *International Journal of Research and Applied Innovations*, 4(4), 5533-5537.
63. Garg, V. K., Soundappan, S. J., & Kaur, E. M. (2020). Enhancement in intrusion detection system for WLAN using genetic algorithms. *South Asian Research Journal of Engineering and Technology*, 2(6), 62-64.
64. Anand, L., Tyagi, R., & Mehta, V. (2024, January). Food recognition using deep learning for recipe and restaurant recommendation. In *Proceedings of Eighth International Conference on Information System Design and Intelligent Applications* (pp. 269-279). Singapore: Springer Nature Singapore.
65. Kumar, A., & Anand, L. (2025). A Novel EEG-Based Deep Learning Framework for Enhancing Communication in Locked-In Syndrome Using P300 Speller and Attention Mechanisms. *KSII Transactions on Internet and Information Systems (TIIS)*, 19(11), 3841-3855.



66. Soundappan, S. J. (2022). AI-Based Fault Detection and Isolation for Reliability in Modern Power Systems. *International Journal of Research Publications in Engineering, Technology and Management (IRPETM)*, 5(4), 7106-7110
67. Chandra, S., Rengarajan, A., Sahoo, G. S., & Sharma⁴, S. (2024, October). Identifying Neuronal Damage and Plasticity by Analyzing Changes in Diffusion Tensor. In *Proceedings of the 5th International Conference on Data Science, Machine Learning and Applications; Volume 2: ICDSMLA 2023, 15–16 December, Hyderabad, India (Vol. 2, p. 433)*. Springer Nature.